Sustainable Food Technology

ROYAL SOCIETY OF CHEMISTRY

PAPER

View Article Online
View Journal

Cite this: DOI: 10.1039/d5fb00584a

Non-equilibrium cold plasma as a sustainable approach to improve functional and thermal properties of pearl and sorghum millet flours

Ritesh Mishra, [a] Sushma Jangra, [b] Abhijit Mishra, [b] Shikha Pandey,[b] Meenu Chhabra[ac] and Ram Prakash [ab]

Received 10th September 2025
Accepted 22nd December 2025

DOI: 10.1039/d5fb00584a

rsc.li/susfoodtech

This study investigates the effects of non-equilibrium cold plasma (NECP) treatment using air plasma and transient exposure methods on the functional, structural, and thermal properties of pearl and sorghum millet flours. Pearl and sorghum millet flours were treated at two different exposure times for 5 min and 10 min, and functional properties such as water and oil holding capacity, water binding capacity, color, and dispersibility of the control and plasma-treated flours were studied. There was no significant difference in the color intensity and the whitening index (WI) with the treatment. However, the 10-minute treatment resulted in an increase in water absorption capacity (1.55–1.81 g g^{-1}), oil absorption capacity (1.21–1.4 g g^{-1}), and water binding capacity (2.25–2.37 g g^{-1}) in pearl millet flour. Similarly, the water absorption capacity (1.43 to 1.74 g g^{-1}), oil absorption capacity (1.08 to 1.27 g g^{-1}), and water binding capacity (2.07–2.26 g g^{-1}) of sorghum millet flour increased with 10 min NECP treatment. In addition, Fourier transform infrared spectrometry analysis detected shifts in functional groups, X-ray diffraction analysis indicated changes in crystallinity, and differential crystallography showed a reduction in gelatinization enthalpy. Overall, plasma treatment can be explored for the development of a process to enhance the functionality of millet flour for applications in food systems.

Sustainability spotlight

Millets are climate-resilient, nutrient-dense grains critical for global food and nutrition security, yet their wider use is limited by processing challenges. Conventional processing often depletes nutrients and demands high energy, contradicting sustainable practices. This study demonstrates the application of non-equilibrium cold plasma (NECP), a non-thermal, chemical-free, and energy-efficient technology, to enhance the functional and thermal properties of pearl and sorghum millet flours without compromising on quality. By improving flour performance for gluten-free and functional food applications, the work promotes sustainable food diversification and supports resilient food systems. This aligns with UN Sustainable Development Goals (SDG 2: Zero Hunger, SDG 3: Good Health and Well-being, and SDG 12: Responsible Consumption and Production).

1. Introduction

Millets, a type of grass, are distinguished by their compact, slender stems and minuscule seeds, both of which exhibit remarkable resistance to extended periods of drought. Millets are considered to be among the earliest cereal grains farmed for the sake of subsistence.[1] Millets are widely known as "smart food." Millets are a highly nutritious food, rich in iron, folate, calcium, zinc, magnesium, phosphorus, copper, vitamins, fiber, and antioxidants. In addition, besides being essential for the proper development and maturation of children, they have been shown to reduce the risk of heart disease and diabetes in adults. In addition, millets are a suitable choice for individuals with coeliac disease or gluten-related illnesses such as wheat allergy and non-celiac gluten sensitivity, which can have significant health consequences when even small amounts of gluten are consumed.[2] There has been a rise in demand for gluten-free products among individuals seeking to adhere to a nutritious diet. To meet this demand, it is imperative to enhance and broaden the food business by advancing the development of ingredients and formulations, as well as increasing the production of functional foods.[3] Sorghum (*Sorghum bicolor*) and pearl millet (*Pennisetum glaucum*) are two significant millet varieties that are renowned for their nutritional advantages and are frequently utilized for producing gluten-free flour. These grains are currently receiving more attention from food scientists, nutritionists, and policymakers because of their socio-economic consequences.[4] To globally promote and popularize these millets, it is essential to create advanced processing techniques that specifically aim to increase the functional and

[a]*Inter-Disciplinary Research Division-Smart Healthcare, Indian Institute of Technology, Jodhpur, Rajasthan, India*

[b]*Department of Physics, Indian Institute of Technology, Jodhpur, Rajasthan, India. E-mail: ramprakash@iitj.ac.in*

[c]*Department of Bioscience and Bioengineering, Indian Institute of Technology, Jodhpur, Rajasthan, India*

structural properties of millet flour. However, the emphasis on the processing and enhancement of millet flours is currently limited due to the lack of awareness regarding their nutritional and health advantages among the population. Meanwhile, various studies have employed boiling, microwave treatment, cooking, and autoclaving for processing.[5] These technologies adversely affect the nutritional properties of the flour. This has highlighted the need to investigate the applicability of non-thermal technologies like cold plasma.

Non-equilibrium cold plasma (NECP) treatment is a highly adaptable method that can be used in various applications in the food industry. It can be used to modify the structure of macromolecules like starch, protein, and cellulose, promote seed germination, eliminate microbes, and extract bioactive chemicals.[6] NECP treatment is an acknowledged non-thermal technology, classified as the fourth state of matter. It is a partially ionized gas that consists of free radicals, photons, ozone, energetic ions, and free electrons in either the ground or excited state.[7–9] The studies reported that the treatment of cold plasma had a significant impact on the functional, rheological, and thermal properties of various types of flour, including wheat flour, quinoa flour, jackfruit seed flour, little millet flour, and bamboo rice flour.[10–15] However, there has been little research conducted on the effects of various treatment conditions on the nutritional and antinutritional components, as well as the functional and thermal properties of millet flours. R. *et al.* (2021)[16] exposed the pearl millet to cold plasma technology at 180 V with a 0.01 m^3 per h airflow rate. The study concluded that the phytic acid content was reduced by 60.66% and 39.27% when the treatment was carried out for 1 and 2 h, respectively. Jaddu, Pradhan *et al.* (2022)[12] reported that the crystallinity of the little millet flour reduces due to the depolymerization of starch during the cold plasma treatment. They also showed that the treatment increased the water absorption capacity (WAC), oil absorption capacity (OAC), swelling capacity, and solubility index of the flour. The impacts of ultra-high pressure coupled with cold plasma treatment on physical, chemical, and digestive qualities are investigated in another research on proso millet starch.[17]

Previous studies on flour properties utilized either a pin-type or a multipin cold plasma setup.[18–22] This device has the capability to generate plasma distributions that are not uniform, resulting in uneven treatment over the surface area. The treatment region for pin-type devices is often confined to the immediate vicinity of the pin electrodes. When dealing with big regions or volumes, it is necessary to either make many passes or use an array of pins, which makes the operation more complex. Attaining a fully homogeneous plasma treatment might be challenging, even with the utilization of several pins. Inconsistent treatment effects can result from variations in plasma intensity among pins. Moreover, the intense concentration of energy around the pin electrodes can lead to localized surface harm or deterioration, particularly for delicate materials. In addition, pin electrodes are prone to experiencing wear and erosion as time passes, which requires frequent maintenance and replacement. This leads to higher operational expenses and periods of inactivity. In contrast to earlier investigations, air plasma is used in our experiment, and the flours can be treated with transient exposure to non-equilibrium cold plasma. The momentary exposure strategy enhances commercial feasibility, as it can be readily integrated into existing flour processing lines without requiring substantial redesign or major infrastructural modifications, making the approach scalable, energy-efficient, and industry-friendly.[23] The transient plasma exposure ensures sufficient interaction between plasma-generated reactive oxygen and nitrogen species (RONS) and flour constituents while minimizing excessive energy input and thermal stress. This short-duration, non-equilibrium treatment helps preserve the intrinsic nutritional and functional attributes of pearl millet flour, while still inducing desirable modifications such as improved hydration behavior, surface activation, and microbial reduction.

During the plasma discharge, the presence of electrons, ions, and excited species leads to their interaction with the surrounding air, resulting in the formation of different reactive oxygen–nitrogen species (RONS).[24] The major species believed to be responsible for these reactive oxygen and nitrogen species (RONS) include atomic oxygen (O), ozone (O_3), hydroxyl radicals (OH), nitric oxide (NO), and hydrogen peroxide (H_2O_2).[25,26] Therefore, this study aimed to examine the effects of NECP treatment on several aspects, including nutritional factors, functional and thermal characteristics, and changes in pearl millet flour (PMF) and sorghum millet flour (SMF). Furthermore, the effects of NECP treatment on several characteristics of PMF and SMF were examined in further detail using principal component analysis to determine the optimal operating parameters. In addition, the use of NECP treatment might be employed to create functional foods and may have motivated the research community to create more sustainable, environmentally friendly, and energy-efficient technologies for millet processing. By improving flour performance for gluten-free and functional food applications, the work promotes sustainable food diversification and supports resilient food systems. This aligns with UN Sustainable Development Goals (SDG 2: Zero Hunger, SDG 3: Good Health and Well-being, and SDG 12: Responsible Consumption and Production).

2. Materials and methods

The pearl millet flour (FMF) and sorghum millet flour (SMF) were obtained from a local market in Jodhpur, Rajasthan, India. The experiments were carried out at ambient temperature in the Cold Plasma Laboratory, located in the Department of Physics at IIT Jodhpur. The analysis was conducted at the Environmental Biotech Lab, located in the Department of Bioscience and Bioengineering at IIT Jodhpur. The functional characteristics, such as Water Holding Capacity (WHC), Oil Holding Capacity (OHC), water binding capacity (WBC), dispersibility, color, foaming capacity (FC), and emulsifying capacity (EC), were evaluated for 5- and 10-minute NECP treatment time using the methodologies described elsewhere.[20,27] Bioactive compounds like total phenolic content (TPC) and total flavonoid content (TFC) were measured according to Mishra *et al.* (2024)[28] with slight modifications. The Fourier transform infrared spectra of millet flours treated with cold plasma were recorded using FTIR

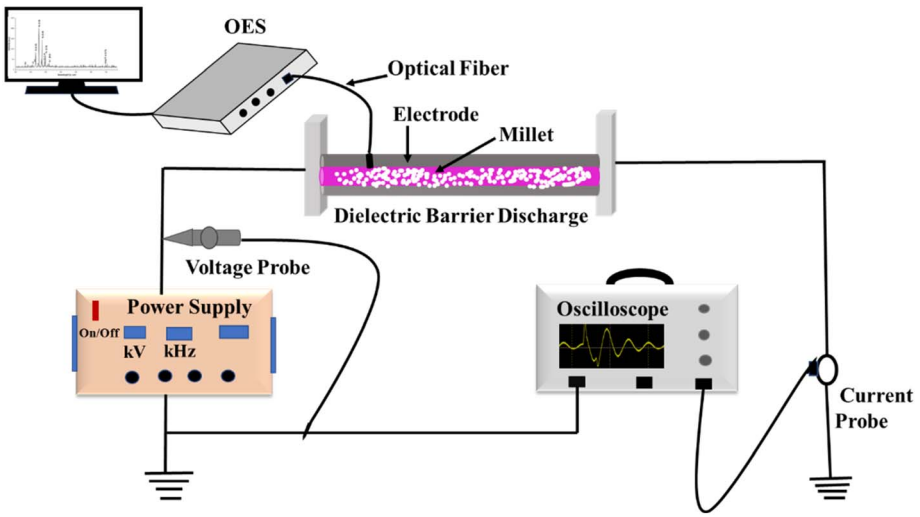

Fig. 1 A schematic illustration of the experimental setup for DBD discharge plasma treatment of millet flour.

spectroscopy (Bruker, Alpha E FTIR, Germany) with attenuated total reflectance (ATR). A PerkinElmer DSC-4000, a differential scanning calorimeter, was employed to determine the peak temperatures of finger millet flour treated with plasma.

2.1 Experimental setup

The experimental setup implemented for the treatment of the millet flour is shown in Fig. 1. The stator and rotator devices are powered by the aforementioned variable bipolar pulsed power supply (Grow controls, GC253HVPS), which is coupled with a high voltage probe (1000×, P6015A, Tektronix) and current monitor (Pearson 110) for monitoring the applied voltage (V) and discharge current (I) waveforms which can be directly visualised by a four-channel digital oscilloscope (MDO3014, 100 MHz, Tektronix). The system consists of a Teflon sleeve rotator connected to an aluminium shaft, which is secured to a holder using a nylon gear wheel to maintain a 1.0 mm distance. The stator is composed of an aluminium shaft of the same size, supplied with an identical gear wheel on two side stands. A 1.5 mm thick hollow dielectric material (dielectric constant: 2.1) was placed over a solid aluminium rod measuring 110 mm in length and 15 mm in diameter to cover the stator electrode that was utilized as the cathode. Another aluminium hollow electrode having the same length and diameter as the first, but inside the hollow electrode, was used as an anode. The same dielectric material was filled similar to the solid aluminium rod. Plasma discharge was produced at atmospheric pressure, and ambient air was used as the gas carrier between the two electrodes. The high voltage (H. V.) probe was linked to the digital oscilloscope, while a wire connector was used to connect the H. V. probe between the high voltage electrode and the power supply. The high-voltage probe was also appropriately grounded. The wire was attached to the grounded electrode of the device and then passed through a current monitor (CT). The output of the CT was then linked to the digital oscilloscope. The study employed Optical Emission Spectroscopy (OES) (Andor Shamrock SR-500i-B1) to investigate the species produced in an air plasma (Fig. 2). Optical emission spectroscopy (OES) was used to examine the gas phase of cold plasma. The spectrum of dielectric barrier discharge under

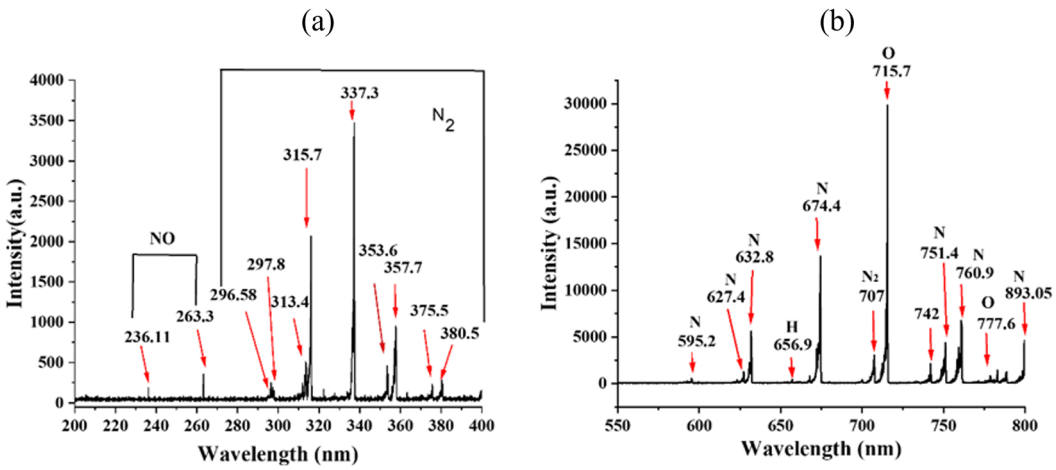

Fig. 2 Optical emission spectrum of DBD plasma at (a) 200 to 400 nm and (b) 550 to 800 nm.

atmospheric pressure plasma is shown in Fig. 2 from 200 to 400 nm and 500 to 900 nm. The spectra from 200 to 400 nm were composed of nitrogen and nitric oxide. NO is produced within the wavelength range of 236 to 283 nm. The spectra were characterised by prominent peaks associated with N_2 second positive system (SPS, C–B) emissions at wavelengths of 315.7, 337.3, 353.6, 357.7, 375.5, and 380.5 nm.[29]

The preliminary experiments were performed to investigate the treatment efficiency at various voltage levels. It was observed that the plasma discharge initiated at a breakdown voltage of 6 kV, stabilized at 7 kV, and remained stable until 9 kV. Due to the impact on the high voltage electrode, it is not suggested to perform prolonged plasma treatments. Moreover, exceeding a specific duration of treatment fails to significantly improve the desired outcomes. Prolonged treatment durations can result in physical harm to the material being treated, including surface erosion, alterations in texture, or compromised structural integrity. Furthermore, when exposed to high voltage for an extended period, the substantial energy released during plasma discharge has the ability to cause nutritional components present in millet flours to deteriorate, including vitamins, amino acids, and antioxidants. Attaining consistent plasma treatment for every individual flour particle can be a challenge. Non-uniform treatment can lead to variations in the quality and functionality of food products. Therefore, we fine-tune our device to achieve the most effective treatment duration. This includes treatment times of up to 20 minutes at 7 kV and up to 10 minutes at 9 kV. In our previous work, we used NECP treatment on finger millet flour at 7 kV and found that higher voltage will increase the crystallinity of the flour, thereby increasing its functionality.[15] Consequently, the parameters selected for the treatment of PMF and SMF were established as 9 kV for a duration of 5–10 minutes.

2.2 Functional properties

The functional properties, including water absorption capacity (WAC), oil absorption capacity (OAC), water binding capacity (WBC), dispersibility, foaming capacity (FC), and emulsifying capacity (EC), were assessed for control as well as NECP-treated pearl millet and sorghum millet flours using the specified methodology.[20,27]

To obtain water binding capacity (WBC), 1.0 g of millet flour samples was combined with 10 mL of deionized water and subjected to centrifugation at 2000 g for 10 min. WBC was calculated using the expression given by Quinton (2002).[30] WBC was determined as the ratio of grams of water retained to grams of solid. The WAC and OAC were determined by employing the methods with minor alterations outlined by Chaple *et al.* (2020).[27] The WAC and OAC were determined using eqn (1).

$$\text{WAC and OAC}\left(\text{g}/\text{g}^{-1}\right) = \frac{\text{Sample weight after centrifugation} - \text{Initial sample weight}}{\text{Initial sample weight}} \quad (1)$$

2.2.1 Emulsifying and foaming capacity. To determine the emulsifying capacity (EC), a solution containing 0.5 grams of millet flour, 5 mL of distilled water, and 5 mL of soybean oil was made in a centrifuge tube. The mixture was mixed using a vortex and then centrifuged at a force of 340 g for 10 minutes. The resulting suspension was carefully transferred to a graduated cylinder, and the total volume as well as the volume of the emulsion layer were precisely measured.

The EC (%) was calculated using eqn (2) as specified by Kheto *et al.* (2022):[31]

$$\text{EC}(\%) = \frac{\text{emulsion volume (mL)}}{\text{total volume (mL)}} \times 100 \quad (2)$$

To measure foaming capacity (FC), 1 gram of millet flour with 50 mL of distilled water was mixed in a beaker. The solution was aggressively stirred for 5 minutes and immediately put into a measuring cylinder. The volume of foam generated was recorded, and FC (%) was determined using eqn (3):

$$\text{FC}(\%) = \frac{\text{volume after shaking(mL)} - \text{inital volume of suspension}}{\text{inital volume of suspension(mL)}} \times 100 \quad (3)$$

2.2.2 Dispersibility. A measured quantity of 10 g of flour was mixed with 100 mL of deionized water, and placed in a 100 mL measuring cylinder. The components were blended and left undisturbed for a duration of 3 hours. The dispersibility of flour was determined by subtracting the volume of settled particles from 100.[32]

2.3 Color

The color values L^*, a^*, b^*, ΔE of PMF and SMF (control and NECP treated) were determined using color reader CR6 (3nh). The L^*, a^*, b^*, ΔE, hue angle, whitening index (WI), yellow index (YI), and browning index (BI) values of PMF and SMF (both control and NECP treated) were determined using eqn (4)–(8) given elsewhere.[33,34]

$$\text{Hue angle}(H) = \tan^{-1}\frac{b}{a} \quad (4)$$

$$\text{Total color difference}(\Delta E) = \sqrt{\Delta L^{*2} + \Delta a^{*2} + \Delta b^{*2}} \quad (5)$$

$$\text{Whitening index(WI)} = \sqrt{(100 - L^*)^2 + a^{*2} + b^{*2}} \quad (6)$$

$$\text{Yellow index(YI)} = \frac{142.86b^*}{L^*} \quad (7)$$

$$\text{Browning index(BI)} = \frac{[100 \times (X - 0.31)]}{0.172} \quad (8)$$

where $X = (a^* + 1.75 \times L^*)/(5.645 \times L^* + a^* - 3.012 \times b^*)$.

2.4 Bioactive compounds

The sample extracts were prepared according to the procedure outlined by Kheto *et al.* (2022).[31] Then the prepared sample

extract was used to estimate the total phenol content (TPC; g of GAE in 100 g of dm) and total flavonoid content (TFC; g of QE in 100 g of dm).

2.5 Fourier transform infrared spectrometry

The FTIR spectra of the PMF and SMF samples were acquired to assess the functional group variations using a FTIR spectrophotometer (Bruker, Alpha E FTIR, Germany) with attenuated total reflectance (ATR). Samples were gently placed on a ZnSe crystal and scanned at 64 scans per sample to obtain % transmittance at specific wavenumbers ranging from 4000 to 400 cm^{-1}.[31]

2.6 Thermal properties

The thermal properties of PMF and SMF samples were determined by a differential scanning calorimeter (PerkinElmer DSC-4000), to determine the peak temperatures of millet flours treated with plasma in the range of 20 to 220 °C at 10 °C per min, as reported by Kheto *et al.* (2022).[31]

2.7 Field emission scanning electron microscopy (FESEM) analysis

The morphology of the PMF and SMF samples was examined using a field emission scanning electron microscope (Thermo Fisher Apreo-2 at a 5 kV acceleration voltage). Before imaging, both control and NECP-treated samples were sputtered with gold using a DC sputter. FESEM imaging was then performed to visualize the microstructural variations.[23]

2.8 X-ray diffractogram analysis

The PMF and SMF samples were analysed using an X-ray diffractometer (Bruker AXS D8 Advance, Germany) to obtain their X-ray diffractograms (XRD). The samples were subjected to an X-ray beam with an intensity of 15 mA and a voltage of 30 kV to investigate the intensity pattern of crystallinity within the 2θ range of 4–45°, using a steep angle of 0.02° and a scan rate of 5/min.[31]

2.9 Antinutritional factors

To evaluate the influence of NECP on antinutritional components in PMF and SMF, both tannins and phytic acid were quantified in untreated and plasma-treated samples. Tannin analysis was carried out following the procedure described by Yadav *et al.* (2021).[35] Briefly, 1 g of flour was extracted using 10 mL of acidified methanol (HCl : methanol = 1 : 100), and centrifuged at 6000 rpm for 20 minutes. Then, 1 mL of extract was mixed with 5 mL of vanillin reagent and allowed to react for 20 minutes. The absorbance of the developed color was then recorded at 500 nm using a UV-visible spectrophotometer (UV-1800, Shimadzu, Japan).

Phytic acid was estimated by the method given by Yadav *et al.* (2021).[35] Briefly, 0.1 g of the sample was extracted using 10 mL of 0.2 mol per L hydrochloric acid and allowed to stand for 1 hour. The mixture was then centrifuged at 5000 rpm for 15 minutes, and later 0.5 mL of the clear supernatant was carefully transferred into a glass-stoppered test tube. An iron(III) reagent was prepared by dissolving 0.2 g of ammonium iron(III) sulfate dodecahydrate in 100 mL of 2 mol per L HCl and diluting to 1 L with distilled water. Accordingly, 1 mL of this reagent was added to the sample and the sample was heated for 30 minutes and subsequently cooled in an ice water bath to 25 °C. Then 2 mL of bipyridine solution (10 g of 2,2′-bipyridine and 10 mL thioglycolic acid in 1 L of distilled water) was added to the test tube. After 1 minute, absorbance was recorded at 519 nm using a UV-vis spectrophotometer (UV-1800, Shimadzu, Japan).

2.10 Statistical analysis

The studies were conducted in triplicate, and the results were provided as the mean standard deviation. The statistical significance was assessed using the Duncan test. In addition, principal component analysis (PCA) was conducted using Origin pro 2023 software from OriginLab, USA, to determine the optimal conditions.

3. Results and discussion

3.1 Plasma characteristics

A typical *V–I* characteristic of the above-described DBD source is shown in Fig. 3. The electric power dissipated into the plasma is calculated from waveforms of applied voltage (U_t) and the discharge current (i_t), using the following relationship.[36]

$$P_{\text{avg}} = \frac{1}{T}\int_0^t P_t \mathrm{d}t \tag{9}$$

where T is the period of oscillation, $P(t)$ is the instantaneous power calculated by multiplying the instantaneous voltage $V(t)$ and current $I(t)$.

The electron density can be approximated from the *V–I* curve using the following relationship:[11]

$$n_e = \frac{J}{e\mu_e E} = \frac{I_{\text{rms}}}{Ae\mu_e E} \tag{10}$$

where J is the current density, A is the cross-sectional area of the powered electrode, I_{rms} is the root mean square current, E is the electric field between the electrodes, e is the electronic charge, and μ_e is the electron mobility, *i.e.*, 552 $cm^2\ V^{-1}\ s^{-1}$ in the case of nitrogen. The operational conditions result in approximately

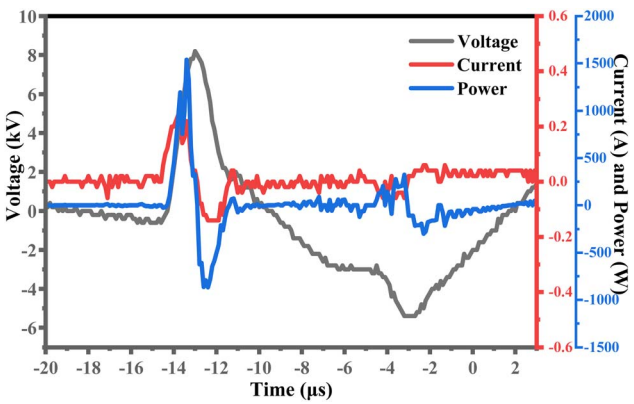

Fig. 3 Typical *V–I* characteristics for DBD 9 kV/20 kHz.

an average power consumption of 10 W and an electron density of 4.19×10^9 particles per cm^3

3.2 Effect of NECP on functional characteristics of millet flour

The functional characteristics of PMF and SMF for control (PMFC and SMFC) and NECP-treated samples for 5 minutes (PMF5 and SMF5) and 10 minutes (PMF10 and SMF10) are presented in Table 1. The functional characteristics of all treated samples were substantially enhanced through NECP-treatment, which was maximum for the 10-minute treated samples. The oil and water absorption capacity of plasma-treated PMF and SMF showed a positive correlation with increasing treatment time. The untreated PMF and SMF exhibited an oil absorption capacity of 1.21 ± 0.041 g g^{-1} and 1.08 ± 0.02 g g^{-1}, and a water absorption capacity of 1.55 ± 0.083 g g^{-1} and 1.43 ± 0.042 g g^{-1}, respectively. The OAC of PMF10 and SMF10 had maximum values of 1.4 ± 0.034 g g^{-1} and 1.27 ± 0.015 g g^{-1}, which were significantly ($P < 0.05$) higher than those of the untreated samples (PMFC and SMFC). Similarly, the WAC of PMF10 and SMF10 had significantly ($P < 0.05$) higher values, 1.81 ± 0.094 and 1.74 ± 0.08, compared to the untreated samples. The increase in OAC and WAC is attributed to the existence of plasma-generated species, such as ions and radicals. These species improve the hydrophilic characteristics of flour, with the degree of starch molecule degradation after NECP treatment contributing to this enhancement.[37] Furthermore, the degradation of starch is mostly attributed to the influence of high-energy plasma species and the partial oxidation of starch, particularly by ozone, resulting in the formation of carboxylic starch. In addition, it is possible that the sample treated with NECP had a higher concentration of hydrophilic sites, including proteins, carbohydrates, and certain residues of polar amino acids. The NECP treatment causes the depolymerization of starch particles, increasing amylose content. This increase in amylose content leads to an increase in crystallinity, which is also associated with increased water absorption capacity. The FTIR results support these findings. Additionally, the NECP treatment causes the formation of fissures and dents, which provide more sites for lyophilic groups. This ultimately leads to an increase in the oil absorption capacity (OAC) of the flour. Similar findings were reported elsewhere.[20,38] However, Chaple *et al.* (2020)[27] noticed that there were no notable changes in the OAC of wheat flour when exposed to 80 kV plasma for durations ranging from 5 to 30 minutes. They observed that the quantities of protein and nonpolar amino acids exhibited fluctuations, although these variations were deemed insignificant. Increased WAC and OAC levels have the intriguing impact of enhancing the volume and texture of baked food products, and this attribute makes them well-suited for various baking purposes.[39]

The water binding capacity (WBC) of NECP-treated flour was enhanced by the plasma treatment, as shown in Table 1. The WBC of the control (PMFC and SMFC) samples was 2.25 ± 0.059 and 2.01 ± 0.007, respectively, which had a significantly higher ($P < 0.05$) value for the 10-minute treated samples. The WBC of PMF10 and SMF10 was determined to be 2.37 ± 0.021 and 2.26 ± 0.055, while for PMF5 and SMF5, the value of WBC was recorded as 2.34 ± 0.016 and 2.11 ± 0.003, respectively. Similarly, Chaple *et al.* (2020)[27] reported that plasma treatment resulted in an enhancement in the water binding capacity (WBC) of flour. The flour's hydration characteristics are enhanced by plasma treatment, indicating that the higher surface area resulting from the initial plasma treatment influences the hydration qualities of the flours. This information can be considered in order to meet specific functional needs.

Furthermore, as compared to the control, the NECP-treated samples showed significantly higher ($P < 0.05$) values for EC and FC. The control PMF and SMF exhibit EC values of $61.86 \pm 0.51\%$ and $61.29 \pm 0.023\%$ (Table 1), respectively. Following a 10-minute plasma treatment, the EC value exhibited a rise to $64.12 \pm 0.635\%$ and $63.21 \pm 0.084\%$. The increase can be ascribed to the improved disorganized arrangement, which allows the proteins to engage with both water and oil. Consequently, the ability of the emulsion to hold and disperse substances is enhanced, and the creation of air bubbles is increased.[40] The FC value of the treated PMF10 and SMF10 significantly increased ($p < 0.05$) to $13.18 \pm 0.282\%$ and $12.19 \pm 0.337\%$, respectively, compared to the control PMFC and SMFC with FC values of $11.57 \pm 0.492\%$ and $10.44 \pm 0.22\%$, respectively. Sarkar *et al.* (2023)[21] observed that the plasma treatment

Table 1 Effect of NECP on functional characteristics of finger millet flour[a]

	PMFC	PMF5	PMF10	SMFC	SMF5	SMF10
Water absorption capacity (WAC) (g g^{-1})	1.55 ± 0.083^{b}	1.68 ± 0.04^{ab}	1.81 ± 0.094^{a}	$1.43 \pm 0.04^{b}2$	1.52 ± 0.1^{b}	1.74 ± 0.08^{a}
Oil absorption capacity (OAC) (g g^{-1})	1.21 ± 0.041^{a}	1.28 ± 0.03^{b}	1.4 ± 0.034^{c}	1.08 ± 0.02^{c}	1.15 ± 0.03^{b}	1.27 ± 0.015^{a}
Water binding capacity (WBC) (g g^{-1})	2.25 ± 0.059^{b}	2.34 ± 0.016^{a}	2.37 ± 0.021^{a}	2.01 ± 0.007^{c}	2.11 ± 0.003^{b}	2.26 ± 0.055^{a}
Total phenol content (TPC) (mg GAE/100 g dm)	2.39 ± 0.08^{NS}	2.34 ± 0.072^{NS}	2.25 ± 0.035^{NS}	2.22 ± 0.04^{b}	2.14 ± 0.03^{ab}	2.09 ± 0.023^{a}
Total flavonoid content (TFC) (mg QE/100 g dm)	2.17 ± 0.092^{NS}	2.16 ± 0.11^{NS}	2.04 ± 0.035^{NS}	1.73 ± 0.05^{b}	1.65 ± 0.031^{b}	1.60 ± 0.023^{a}
Emulsifying capacity (EC)%	61.86 ± 0.51^{b}	62.38 ± 0.21^{b}	64.12 ± 0.635^{a}	61.29 ± 0.023^{c}	62.33 ± 0.087^{b}	63.21 ± 0.084^{a}
Foaming capacity (FC)%	11.57 ± 0.492^{b}	12.39 ± 0.385^{ab}	13.18 ± 0.282^{a}	10.44 ± 0.22^{c}	11.11 ± 0.217^{b}	12.19 ± 0.337^{a}
Dispersibility%	79.02 ± 0.921^{b}	76.81 ± 0.737^{ab}	74.13 ± 1.11^{a}	77.78 ± 0.683^{c}	74.29 ± 0.858^{b}	71.46 ± 0.51^{a}

[a] Means with different superscripts in the same row represent significant ($p < 0.05$) differences with each other.

Table 2 Effect of NECP on the color of pearl and sorghum millet flour[a]

Color index	PMFC	PMF5	PMF10	SMFC	SMF5	SMF10
L^*	46.01 ± 0.02^{NS}	46.035 ± 0.015^{NS}	46.325 ± 0.175^{NS}	47.525 ± 0.015^{a}	47.30 ± 0.01^{b}	47.395 ± 0.015^{b}
a^*	0.635 ± 0.005^{NS}	0.655 ± 0.01^{NS}	0.625 ± 0.035^{NS}	0.855 ± 0.005^{b}	0.82 ± 0.01^{b}	0.88 ± 0.01^{a}
b^*	0.855 ± 0.005^{a}	0.825 ± 0.015^{b}	0.835 ± 0.035^{b}	1.685 ± 0.045^{a}	1.475 ± 0.005^{b}	1.495 ± 0.015^{b}
Hue angle (h^*)	1.574 ± 0.012^{NS}	1.818 ± 0.033^{NS}	1.605 ± 0.089^{NS}	1.227 ± 0.0075^{a}	1.229 ± 0.01^{b}	1.136 ± 0.012^{c}
Whitening index (WI)	45.99 ± 0.02^{NS}	46.02 ± 0.015^{NS}	46.314 ± 0.174^{NS}	47.491 ± 0.016^{a}	47.282 ± 0.01^{b}	47.366 ± 0.014^{b}
Yellow index (YI)	2.654 ± 0.016^{a}	2.56 ± 0.047^{b}	2.574 ± 0.098^{b}	5.065 ± 0.136^{a}	4.453 ± 0.015^{b}	4.512 ± 0.043^{b}
Browning index (BI)	2.826 ± 0.019^{a}	2.627 ± 0.048^{b}	2.748 ± 0.048^{b}	4.763 ± 0.089^{a}	4.343 ± 0.01^{b}	4.469 ± 0.015^{b}
Color change ΔE	0.11 ± 0.01^{c}	0.17 ± 0.01^{b}	0.29 ± 0.014^{a}	2.525 ± 0.05^{a}	2.255 ± 0.015^{b}	2.335 ± 0.025^{b}

[a] Means with different superscripts in the same row represent significant ($p < 0.05$) differences from each other.

of the pearl millet surface leads to the exposure of hydrophobic groups, which in turn attract oil droplets and enhance the stability of the emulsions formed. In addition, the plasma treatment may have raised the surface elasticity; this higher elasticity allows the protein to stretch and deform around the oil droplets and air bubbles, resulting in an enhanced FC.[41] The NECP treatment did not affect the dispersibility of the PMF and SMF samples. Similar findings were reported elsewhere.[12]

3.3 Bioactive compounds (total phenol content and total flavonoid content)

The NECP treatment did not have a significant impact on the values of total phenolic content (TPC) and total flavonoid content (TFC), as shown in Table 1. The TPC of the PMFC was determined to be 2.39 ± 0.08 (mg GAE/100 g dm). The TPC decreased as the treatment duration increased from 5 to 10 minutes. The TFC of the PMFC sample was 2.17 ± 0.092 (mg QE/100 g dm), which decreased with the NECP treatment. Similarly, the TFC of SMFC was measured to be 2.22 ± 0.04, which reduces to 2.14 ± 0.03 and 2.09 ± 0.023 ($p < 0.05$) for SMF5 and SMF10, respectively. The TFC has also decreased after NECP treatment, which was recorded as 1.65 ± 0.031 for SMF5 and 1.60 ± 0.023 for SMF10, whereas the untreated sample (SMFC) had a TFC value of 1.73 ± 0.05. The minor decline in TPC (Total Phenolic Content) and TFC (Total Flavonoid Content) indicates that plasma discharge generates high-energy electrons that, through direct interaction with phenolic compounds, induce the dissociation of oxygen molecules and subsequently lead to deterioration.[10,12] Furthermore, a decrease in phenolic compounds can potentially contribute to the generation of ozone and other reactive species through dissociation, a process in which individual oxygen atoms unite with oxygen molecules to produce ozone. Conversely, aliphatic molecules, such as hydroxylated and quinone compounds, are produced through the reaction of molecular ozone with the aromatic rings of phenolics, leading to the breakdown and deterioration of phenolic compounds.[21] Additional investigation is required to comprehend the interaction between phytochemicals and reactive species. Overall, the recent findings corroborated the results of the previous study by Sarkar *et al.* (2023) and Almeida *et al.* (2015),[21,42] which revealed a decrease in phytochemicals following CP treatment.

3.4 Effect of NECP on color

The color attributes of cold plasma-treated and untreated PMF and SMF were assessed and reported in Table 2. The results were derived using the CIELAB (L^*, a^*, b^*) color space. L^* represents lightness, while a^* and b^* represent red-greenness and blue-yellowness, respectively.[43] The L^* value of PMF samples varied between 46.01 ± 0.02 and 46.325 ± 0.175. The flour experienced no reduction in its L^* value following the NECP treatment. This shows that NECP treatment has no effect on L^* values, indicating similar hues for the treated and untreated PMF samples. The values a^* and b^* of all the samples range from 0.635 ± 0.005 to 0.625 ± 0.035 and from 0.855 ± 0.005 to 0.825 ± 0.015, respectively. The L^* value of the SMF samples ranged from 47.525 ± 0.015 to 47.395 ± 0.015. The NECP treatment did not cause any decrease in the L^* value of the flour. The results demonstrate that NECP treatment does not impact the L^* values, indicating that the hues of the treated and untreated SMF samples are similar. The values of a^* and b^* for all the samples vary between 0.855 ± 0.005 and 0.88 ± 0.01, and between 1.685 ± 0.045 and 1.495 ± 0.015, respectively. The lack of significant shifts in color values implies that non-equilibrium cold plasma does not induce any changes in the product's color. The whitening index (WI), yellow index (YI), and hue angle (h^*) of the plasma-treated pearl millet flour remain

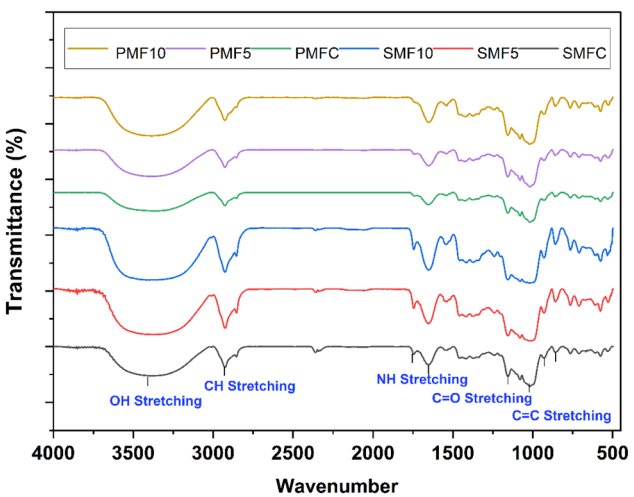

Fig. 4 FTIR spectra of PMF and SMF treated with NECP.

Table 3 Effect of NECP on thermal properties and crystallinity of pearl millet and sorghum millet flour

	T_o °C	T_p °C	T_c °C	ΔH J g^{-1}	Degree of gelatinization%	% Crystallinity%
PMFC	32.23	101.8	175.25	194.93	NA	26.48
PMF5	31.23	98.85	168.25	153.85	21.07%	29.34
PMF10	29.56	93.53	166.92	150.72	22.07%	31.4
SMFC	38.56	87.79	150.07	182.76	NA	25.38
SMF5	36.73	86.53	157.06	151.53	17.08%	27.187
SMF10	34.4	76.37	162.23	140.37	23.15%	28.635

unchanged with the different treatment times. However, there was only a minor overall change in color observed, and this shift can be attributed to the surface structure of the particles, which is significantly affected by plasma and is evident in the optical characteristics of flour. Due to the surface etching caused by plasma treatment, it is expected that there would be changes in the color values of the treated product.[13]

3.5 Fourier transmission infrared spectrum of millet flour

The FTIR spectra of control and NECP-treated PMF and SMF samples are shown in Fig. 4. The FTIR spectra depicted the C–H stretching vibration, the starch functional groups (O–H), and the glucose pyranose vibrational twisting patterns in specific locations, namely 2800–3000 cm^{-1}, 3000–3600 cm^{-1}, and 800–1200 cm^{-1}. The range of 1600–1700 cm^{-1} is used to indicate the stretching of the C–O bond, while the range of 1500–1600 cm^{-1} is used to indicate the vibration of the N–H bond. The difference in absorbance observed between the PMF and SMF samples could indicate a change in functional group concentration due to complexity in their structure. All treated and control samples had a similar absorbance pattern, indicating that no new functional groups had formed in the sample; however, there was a difference in the intensity of NECP-treated samples due to the interaction with free radicals generated during the course of cold plasma.[14] The FTIR spectra of PMF and SMF subjected to treatments of 5 and 10 minutes displayed clearly identifiable peaks, as depicted in the figure. The sample exhibited a prominent peak at a wavenumber of 3391 cm^{-1}. This peak elongated in the treated samples, which is associated with the elongation of OH bonds. The glycosidic bonds of the starch molecules are being attacked by reactive oxygen and nitrogen species (RONS), which provide powerful intermolecular interactions *via* RONS found in the cold plasma.[21] The breakdown of starch components is caused by these bonds, which demonstrate C–H stretching at 2926 and 2849 cm^{-1}. The analysis revealed further peaks at 1746, 1547, 1650, 1162, and 1012 cm^{-1}, corresponding to the primary amide, secondary amide of C–O stretching, C–C stretching, and alkene group of C–C bending, respectively. Zhou *et al.* (2018)[44] reported the presence of absorption peaks at 1167 cm^{-1}, 1079 cm^{-1}, and 994 cm^{-1}. Similarly, Chaple *et al.* (2020)[27] found analogous peaks in the region of 1600–1700 cm^{-1}. These data suggest that the starch granules underwent oxidation as a result of the influence of plasma species.[10,12] In addition, the transmittance in the 800–1200 cm^{-1} band for the sample shows an increase compared to the control, indicating alterations in the crystallinity of starch granules and the promotion of more organized C–O–C arrangements. The carbonyl groups (C=O) are produced through the oxidation of hydroxyl (OH) groups in starch by reactive oxygen species (ROS) created during cold plasma treatment.[22]

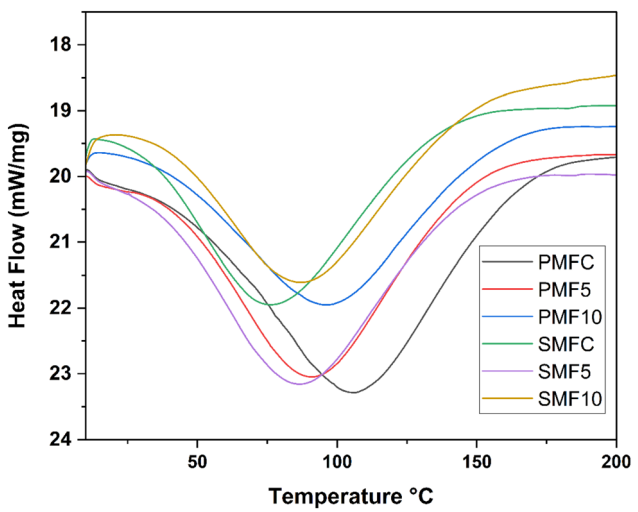

Fig. 5 Thermograph of untreated and NECP-treated PMF and SMF.

3.6 Thermographs of millet flour

Table 3 summarizes the thermal properties of both the control and NECP-treated samples, which include the onset temperature (T_o), peak temperature (T_p), and conclusion temperature (T_c). Thermographs of treated and control PMF and SMF are shown in Fig. 5. The changes in the physical state and crystalline structure of flour can be caused by either absorbing heat (endothermic) or releasing heat (exothermic). The gelatinization temperatures of samples treated with PMF and SMF were somewhat lower in comparison to the untreated samples. The NECP-treated samples exhibited an earlier onset temperature (T_o) compared to the untreated ones. This can be due to a higher level of damage caused by plasma species to the molecular structure of starch. The peak temperature (T_p) of the PMFC was 101.8 °C. In the PMF5 sample, the peak temperature decreased to 98.85 °C, while in the PMF10 sample, it decreased further to 93.53 °C. Similarly, the peak temperature (T_p) of the SMF5 and SMF10 decreased to 86.53 and 76.37 °C, respectively, compared to the SMFC, which had a temperature of 87.79 °C. Thirumdas *et al.* (2017)[45] reported a comparable reduction in the gelatinization temperature of rice starch following cold plasma treatment. This endothermic shift is associated with the depolymerization or alteration in the ratio of amylose and amylopectin in starch granules and complete

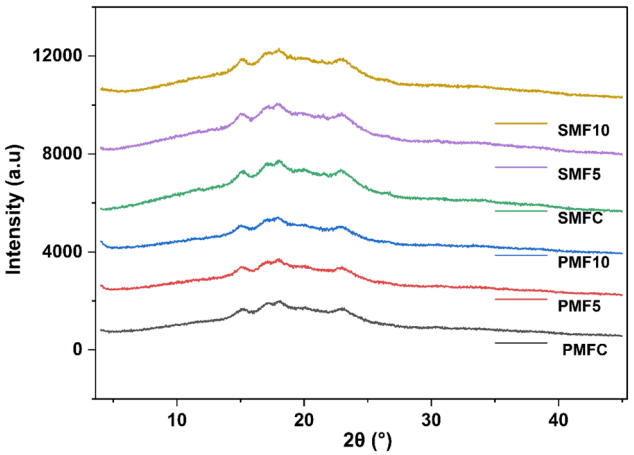

Fig. 6 Diffractograms of untreated and NECP-treated PMF and SMF.

degradation of the starch crystalline structure by NECP-generated species.[46] Similarly, the peak temperatures were decreased for little millet flour treated with multipin cold plasma employing varying power and treatment time.[20] However, Sarkar *et al.* (2023)[21] reported that the pearl millet flour samples subjected to cold plasma exhibited a slightly elevated peak temperature (T_p), which could be attributed to the formation of cross-links induced by plasma species. Wongsagonsup *et al.* (2014)[47] previously documented that the lower plasma power levels cause the plasma species to start the process of connecting starch chains, whereas greater plasma power levels result in the breakdown of starch chains. In our earlier research, we observed that the peak gelatinization temperature increases while using low-power plasma. Therefore, in this investigation, we treated all the samples by applying a higher voltage of approximately 9 kV. The gelatinization enthalpy (ΔH) decreases slightly from 194.93 J g^{-1} to 153.85 J g^{-1} in PMF5 and 150.72 J g^{-1} in PMF10. Similarly, gelatinization enthalpy (ΔH) is reduced to 151.53 J g^{-1} and 140.37 J g^{-1} in SMF5 and SMF10, as compared to untreated SMF, which had a gelatinization enthalpy of 182.76 J g^{-1}. The PMF10 and SMF10 resulted in a significant reduction in the gelatinization enthalpy, with a maximum decrease of 22.67% and 23.17%, respectively. The reduction in enthalpy indicates that the millet flour treated with non-equilibrium cold plasma requires less energy for gelatinization.

3.7 Effect of NECP on structural properties of millet flour

Fig. 6 illustrates the XRD spectrum used to examine the effect of NECP treatment on the crystal structure of PMF and SMF. The spectra clearly demonstrate the presence of semicrystalline areas in both the PMF and SMF, characterized by a closely packed and organized arrangement of starch molecules. The X-ray diffraction (XRD) patterns of the millet flour samples exhibited wide peaks, suggesting the presence of a type-A crystalline pattern, which is evident from the prominent peaks at 2θ values of 15.14°, 17.12°, 17.94°, 20.04°, 22.94°, and 26.52°. Furthermore, there are dispersed peaks that signify the existence of non-crystalline areas. The crystallinity percentage in PMF increases with NECP treatment, which was 26.48% in PMFC and increased to 29.34% and 31.4% in PMF5 and PMF10, respectively (Table 3). Similarly, the level of crystallinity in SMF5 (27.18%) and SMF10 (28.63%) was higher than that of the SMFC (25.38%). The increase in crystallinity is attributed to the deterioration of non-crystalline portions of starch molecules caused by NECP treatments. The NECP treatment may have caused alterations in starch granules, such as breakdown and depolymerization, due to interactions with RONS. Moreover, reactive plasma species clash with starch constituents such as amylose and amylopectin, resulting in an increase in the number of sites accessible for starch–water interaction and, consequently, an increase in the water solubility index.[48] Kaur & Annapure (2024)[49] reported that the impact of atmospheric cold plasma on finger millet resulted in an increase in relative crystallinity and subsequently led to an increase in the water solubility index. Therefore, NECP-treated samples led to the creation of starches that exhibited greater stability and solubility in comparison to the control.

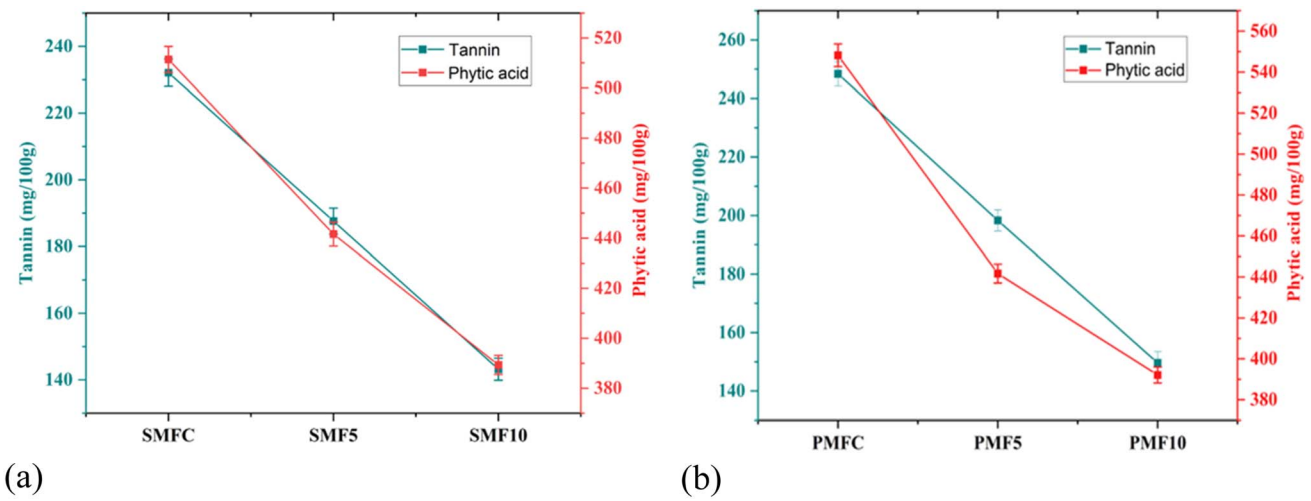

Fig. 7 Tannin and phytic acid in untreated and NECP-treated (a) SMF and (b) PMF.

3.8 Effect of NECP on antinutritional factors

The effect of NECP treatment on antinutritional factors in PMF and SMF is illustrated in Fig. 7, showing a progressive and significant reduction in both tannin and phytic acid content with increasing treatment time (0, 5, and 10 minutes). In PMF, the tannin content decreased from approximately 250 mg/100 g to 145 mg/100 g, and phytic acid content reduced from 545 mg/100 g to 395 mg/100 g. Similarly, in SMF, tannin content declined from 232 mg/100 g to 143 mg/100 g, while phytic acid content decreased from 511 mg/100 g to 368 mg/100 g. These results indicate a dose-dependent degradation of antinutritional compounds, attributed to the action of plasma-generated RONS such as hydroxyl radicals ($^{\bullet}OH$), ozone (O_3), nitric oxide (NO), and peroxynitrite ($ONOO^-$), which are known to induce oxidative cleavage of phenolic and phosphate-rich compounds.[50] Similar observations were reported by Kheto *et al.* (2023),[40] where atmospheric pressure cold plasma treatment significantly reduced phytic acid and improved protein digestibility in guar seed flour. Likewise, R. L. *et al.* (2021)[16] demonstrated that cold plasma exposure decreased phytic acid content in pearl millet by up to 60.66%, attributing the effect to oxidative breakdown of phytate rings and possible activation of endogenous phytase enzymes. In another study, Pankaj *et al.* (2018)[51] emphasized the ability of plasma to disrupt antinutritional factors in legumes and cereals without compromising the structural integrity of starch and protein fractions. The parallel downward trends of tannins and phytic acid in the current study suggest that both compounds are similarly susceptible to oxidative degradation, supporting the hypothesis that cold plasma can act as a non-thermal, residue-free processing tool for improving the nutritional and functional properties of millet flours. The minimal variability observed in replicates (indicated by small error bars) confirms the reproducibility and consistency of the treatment. These findings validate NECP as a sustainable and scalable intervention for enhancing millet flour quality, especially for applications in functional food formulations where digestibility and mineral bioavailability are critical.

3.9 Principal component analysis

The study examined the correlations between the functional, bioactive chemicals, color, and thermal properties using Principal Component Analysis (PCA). The results revealed two principal components, PC1 (57.33%) and PC2 (37.09%), which accounted for a total of 94.42% of the overall variation (Fig. 8). None of the variables are directly related to any PCs. The untreated samples of SMFC and PMFC were located in the lower left and right quadrants, respectively, indicating disparities in the characteristics of the SMF and PMF samples. While NECP treated SMF10, SMF5, and PMF10, the samples were positioned in the upper left and right quadrants, which suggests notable variations in characteristics compared to the untreated samples. This suggests that a prolonged period of plasma treatment, specifically 10 minutes, is required for the plasma-generated reactive oxygen and nitrogen species (RONS) to sufficiently engage with the flour and influence the functionality of the treated samples.

While these results highlight the promise of NECP as an emerging alternative to conventional thermal processing, still there are certain challenges. The generation and distribution of reactive species can fluctuate depending on humidity, gas composition, and processing distance and may affect reproducibility. Potential oxidative changes to lipids or sensitive bioactive

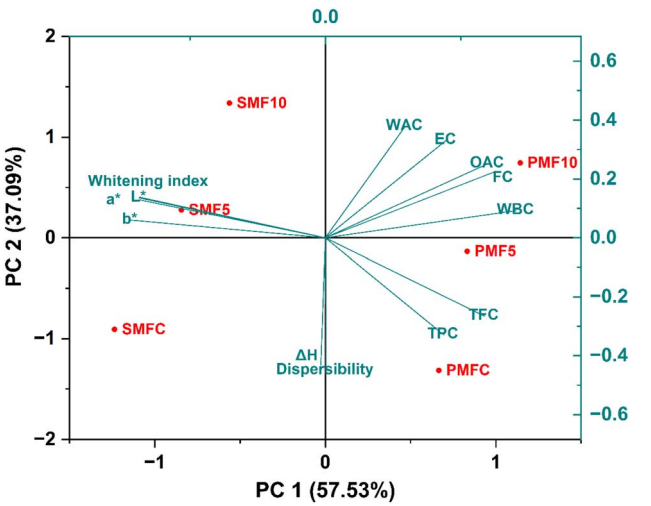

Fig. 8 Biplot of PCA analysis of NECP-treated pearl sorghum millet flour.

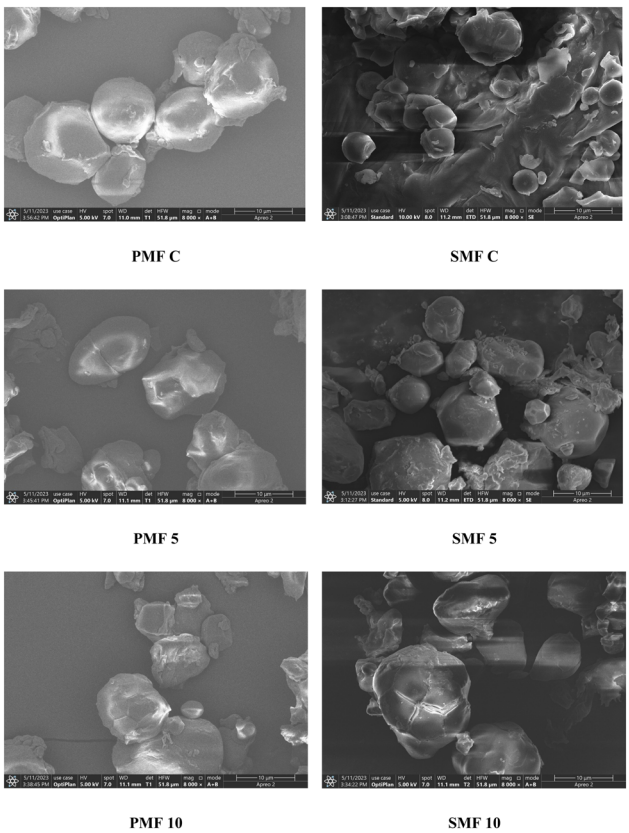

Fig. 9 FESEM images of NECP-treated PMF and SMF.

components may also occur under prolonged exposure, which raises questions regarding long-term storage stability. Lack of established treatment protocols, limited continuous-processing designs, and the requirement for energy-efficiency evaluation are additional obstacles to industrial-scale implementation. Therefore, although NECP demonstrates strong potential for quality enhancement of millet flours, further research is required to address these constraints, particularly by investigating long-term shelf stability, optimizing process uniformity, and validating its technological applicability across diverse food matrices. In addition, further study is required to confirm the suitability of the NECP treatment to improve the functionality of the millet flour.

3.10 Effect on microstructural changes

The microstructural changes induced by NECP treatment in PMF and SMF were examined using FESEM and are shown in Fig. 9. The control samples exhibited compact, well-defined starch granules with smooth, intact surfaces, reflecting minimal structural disturbance. In contrast, the NECP-treated samples showed noticeable morphological alterations, with the degree of surface disruption increasing progressively with treatment duration. For the 5-minute NECP treatment (PMF5 and SMF5), the granules began to show subtle surface roughening, shallow pits, and minor fissures. These features suggest that the initial stage of etching is caused by plasma-generated reactive species. The interaction of ions, radicals, and excited molecules with the granule surface likely resulted in partial removal of the outer layers and weakening of amorphous regions. The effect was more pronounced in the 10-minute treated samples (PMF10 and SMF10), where the granules displayed significant erosion, deeper cracks, and hollowed regions. Such extensive disruption indicates increased penetration of plasma ions into the granular matrix, leading to degradation of amorphous domains and destabilization of the surface architecture. The stronger etching at longer exposure times is consistent with intensified interaction of RONS with starch and protein components.

The FESEM observations are well supported by the structural and thermal transitions reflected in the XRD and DSC analyses. The progressive surface erosion, fissures, and granular disruption seen in NECP-treated PMF and SMF correspond with the increase in relative crystallinity observed in the XRD patterns. The breakdown of amorphous regions by plasma-generated reactive species likely facilitated the reorganization of remaining starch chains into more ordered crystalline domains, as reflected by the higher crystallinity values in PMF10 and SMF10. This structural rearrangement also aligns with the decrease in gelatinization enthalpy (ΔH) and the shift toward lower onset and peak gelatinization temperatures in the DSC thermograms. These findings are consistent with earlier studies reporting that cold plasma exposure causes surface etching, deformation of granules, and the development of cavities in starch and protein-based systems.[52–54] The microstructural breakdown observed in PMF10 and SMF10 supports the enhanced functional and thermal properties discussed earlier, as plasma-induced surface roughness and fissures increase the accessibility of hydrophilic and hydrophobic sites, thereby influencing absorption, gelatinization, and solubility behaviour.[55]

4. Conclusions

This study illustrates the efficiency of non-equilibrium cold plasma treatment using a DBD source made of a stator and a rotator electrode arrangement. These features enable easy scalability and enhance commercial viability without requiring significant redesign. The application of NECP treatment to pearl and sorghum millet flours resulted in notable changes to their functional and physical properties. Specifically, the treatment led to a decrease in dispersibility, alongside increases in oil holding capacity, water holding capacity, and water binding capacity. Importantly, no color changes were observed post-treatment. The increase in peak gelatinization temperature is attributed to the depolymerization of starch molecules induced by the plasma treatment. Overall, the enhanced functional properties of pearl and sorghum millet flours post-NECP treatment suggest their potential as potent components for novel food formulations, such as breads, porridges, and frozen foods. NECP emerges as a promising alternative to traditional heat processing methods, offering a means to improve the quality of millet flour without compromising its physical properties. These findings highlight the potential of NECP to alter the physical and functional characteristics of millet flour, making it a potent component for the food industry.

However, further research is necessary to validate the suitability of plasma-treated millet flour for broader applications within the food industry.

Author contributions

Ritesh Mishra – wrote the original draft, contributed to review and editing, and was responsible for visualization, software, methodology, investigation, formal analysis, data curation, and conceptualization. Sushma Jangra – methodology, formal analysis, and investigation. Abhijit Mishra – methodology, investigation, and data curation. Shikha Pandey – methodology and data curation. Meenu Chhabra – review and editing, conceptualization, and supervision. Ram Prakash – review and editing, visualization, conceptualization, and supervision.

Conflicts of interest

The authors declare that they have no conflict of interest.

Data availability

All the data is presented within the manuscript itself.

Acknowledgements

The authors gratefully acknowledge the CRDSI and the AIOT, IIT Jodhpur, for providing the facilities, technical support, and instrumentation required to carry out this research.

References

1 P. Panwar, A. Dubey and A. K. Verma, Evaluation of nutraceutical and antinutritional properties in barnyard and finger millet varieties grown in Himalayan region, *J. Food Sci. Technol.*, 2016, **53**(6), 2779–2787.
2 V. Falguera, N. Aliguer and M. Falguera, An integrated approach to current trends in food consumption: Moving toward functional and organic products?, *Food Control*, 2012, **26**(2), 274–281.
3 P. Conte, Technological and Nutritional Challenges, and Novelty in Gluten-Free Breadmaking: a Review, *Pol. J. Food Nutr. Sci.*, 2019, **69**(1), 5–21.
4 T. J. Joshi, S. M. Singh and P. S. Rao, Novel thermal and non-thermal millet processing technologies: advances and research trends, *Eur. Food Res. Technol.*, 2023, **249**(5), 1149–1160.
5 L. Yousaf, D. Hou, H. Liaqat and Q. Shen, Millet: A review of its nutritional and functional changes during processing, *Food Res. Int.*, 2021, **142**, 110197.
6 R. Mishra, M. Chhabra and R. Prakash, Non-equilibrium cold plasmas and their impacts on physico-chemical properties of food items, *Rev. Mod. Plasma Phys.*, 2025, **9**(1), 16.
7 S. Jangra, R. Mishra, A. Mishra, S. Pandey and R. Prakash, Analysis of short-term treatment effects of dielectric barrier discharge plasma to improve germination characteristics of wheat seeds, *Radiat. Eff. Defects Solids*, 2024, **179**(7–8), 1023–1031.
8 R. Mishra, S. Pandey, S. Jangra, A. Mishra, M. Chhabra and R. Prakash, Effective microbial control, enhancing antioxidant activity and pesticide removal in fresh cut apples with plasma activated water, *Postharvest Biol. Technol.*, 2025, **228**, 113660.
9 S. Pandey, R. Jangra, K. Ahlawat, R. Mishra, A. Mishra and S. Jangra, Selective generation of nitrate and nitrite in plasma activated water and its physicochemical parameters analysis, *Phys. Lett. A*, 2023, **474**, 128832, DOI: 10.1016/j.physleta.2023.128832.
10 N. N. Misra, S. Kaur, B. K. Tiwari, A. Kaur, N. Singh and P. J. Cullen, Atmospheric pressure cold plasma (ACP) treatment of wheat flour, *Food Hydrocolloids*, 2015, **44**, 115–121.
11 S. Jangra, R. Mishra, A. Mishra, S. Pandey and R. Prakash, Enhancing Physicochemical and Functional Properties of Wheat Flour by Dielectric Barrier Discharge Plasma Treatment, *ACS Food Sci. Technol.*, 2025, **13**, 1459–1468.
12 S. Jaddu, R. C. Pradhan and M. Dwivedi, Effect of multipin atmospheric cold plasma discharge on functional properties of little millet (Panicum miliare) flour, *Innovative Food Sci. Emerging Technol.*, 2022, **77**, 102957.
13 J. K Joy, R. G. T. Kalaivendan, G. Eazhumalai, S. P. Kahar and U. S. Annapure, Effect of pin-to-plate atmospheric cold plasma on jackfruit seed flour functionality modification, *Innovative Food Sci. Emerging Technol.*, 2022, **78**, 103009.
14 L. Zare, N. Mollakhalili-Meybodi, H. Fallahzadeh and M. Arab, Effect of atmospheric pressure cold plasma (ACP) treatment on the technological characteristics of quinoa flour, *LWT–Food Sci. Technol.*, 2022, **155**, 112898.
15 R. Mishra, S. Jangra, A. Mishra, S. Pandey, R. Prakash and M. Chhabra, Enhancement of structural and functional characteristics of millet flours using non-equilibrium cold plasma, *Radiat. Eff. Defects Solids*, 2024, **179**(7–8), 881–887.
16 L. Ramireddy, S. P. Shashikanthalu and M. Radhakrishnan, Improvement in Millet Soaking by Way of Bubbled Cold Plasma Processed Air Exposure; Phytic Acid Reduction Cum Nutrient Analysis Concern, *Front. Adv. Mater. Res.*, 2021, **30**, 1–16.
17 X. Sun, A. S. M. Saleh, Y. Lu, Z. Sun, X. Zhang and X. Ge, Effects of ultra-high pressure combined with cold plasma on structural, physicochemical, and digestive properties of proso millet starch, *Int. J. Biol. Macromol.*, 2022, **212**, 146–154.
18 M. Rao and K. Akhil, Effect of microwave treatment on physical and functional properties of foxtail millet flour, *Int. J. Chem. Stud.*, 2021, **9**(1), 2762–2767.
19 S. Jaddu, S. Abdullah, M. Dwivedi and R. C. Pradhan, Multipin cold plasma electric discharge on hydration properties of kodo millet flour: Modelling and optimization using response surface methodology and artificial neural network – Genetic algorithm, *Food Chem.:Mol. Sci.*, 2022, **5**, 100132.
20 S. Jaddu, R. C. Pradhan and M. Dwivedi, Effect of multipin atmospheric cold plasma discharge on functional properties of little millet (*Panicum miliare*) flour, *Innovative Food Sci. Emerging Technol.*, 2022, **77**, 102957.
21 A. Sarkar, T. Niranjan, G. Patel, A. Kheto, B. K. Tiwari and M. Dwivedi, Impact of cold plasma treatment on nutritional, antinutritional, functional, thermal, rheological, and structural properties of pearl millet flour, *J. Food Process Eng.*, 2023, **46**(5), 14317.
22 V. Sharma, M. S. Tomar, S. Sahoo and R. C. Pradhan, Development of barnyard millet flour rich in bioactive compounds with enhanced functional properties by application of multipin atmospheric cold plasma, *J. Food Process Eng.*, 2024, **47**(6), 14667.
23 S. Jangra, A. Mishra, R. Mishra, S. Pandey and R. Prakash, Transformative impact of atmospheric cold plasma on mung bean seeds: Unveiling surface characteristics, physicochemical alterations, and enhanced germination potential, *AIP Adv.*, 2024, **14**(7), 075215.
24 A. Mishra, R. Mishra, Y. H. Siddiqui, S. Jangra, S. Pandey and R. Prakash, Analysis of discharge parameters of an Argon Cold Atmospheric Pressure Plasma Jet and its impact on surface characteristics of White Grapes, *Phys. Scr.*, 2024, 105615.
25 P. Attri, K. Ishikawa, T. Okumura, K. Koga and M. Shiratani, Plasma Agriculture from Laboratory to Farm: A Review, *Processes*, 2020, **8**(8), 1002.
26 S. Pandey, R. Mishra, A. Mishra, S. Jangra and R. Prakash, Plasma Activated Water Generation in Pin-to-Plate Gas

Phase DBD-based Plasma Source for Enhanced Biochemical Activity, *Phys. Lett. A*, 2025, 130245.
27 S. Chaple, C. Sarangapani, J. Jones, E. Carey, L. Causeret and A. Genson, Effect of atmospheric cold plasma on the functional properties of whole wheat (*Triticum aestivum* L.) grain and wheat flour, *Innovative Food Sci. Emerging Technol.*, 2020, **66**, 102529.
28 R. Mishra, A. Mishra, S. Jangra, S. Pandey, M. Chhabra and R. Prakash, Process parameters optimization for red globe grapes to enhance shelf-life using non-equilibrium cold plasma jet, *Postharvest Biol. Technol.*, 2024, **210**, 112778.
29 A. Mishra, S. Jangra, R. Mishra, S. Pandey, P. Soundharrajan and S. P. Kombade, Characterization Study of a Helium Cold Atmospheric-Pressure Plasma Jet and Its Application in Plasma-Mediated Root Canal Irrigation, *IEEE Trans. Radiat. Plasma Med. Sci.*, 2025, 1.
30 L. Quinton, American Association of Cereal Chemists Approved Methods, 10th ed., CD-ROM American Association of Cereal Chemists, *Carbohydr. Polym.*, 2002, (4), 515.
31 A. Kheto, D. Joseph, M. Islam, S. Dhua, R. Das and Y. Kumar, Microwave roasting induced structural, morphological, antioxidant, and functional attributes of Quinoa (*Chenopodium quinoa* Willd), *J. Food Process. Preserv.*, 2022, **46**(5), 16595.
32 K. D. Kulkarni, D. N. Kulkarni and U. M. Ingle, Sorghum Malt-Based Weaning Food Formulations: Preparation, Functional Properties, and Nutritive Value, *Food Nutr. Bull.*, 1991, **13**(4), 1–7.
33 P. B. Pathare, U. L. Opara and F. A. J. Al-Said, Colour Measurement and Analysis in Fresh and Processed Foods: A Review, *Food Bioprocess Technol.*, 2013, **6**(1), 36–60.
34 H. M. Ali, A. M. El-Gizawy, R. E. I. El-Bassiouny and M. A. Saleh, The role of various amino acids in enzymatic browning process in potato tubers, and identifying the browning products, *Food Chem.*, 2016, **192**, 879–885.
35 S. Yadav, S. Mishra and R. C. Pradhan, Ultrasound-assisted hydration of finger millet (*Eleusine Coracana*) and its effects on starch isolates and antinutrients, *Ultrason. Sonochem.*, 2021, **73**, 105542.
36 A. Mishra, P. S, P. Kumar and R. Prakash, Comparative analysis of disinfection effectiveness of Helium CAP jet, sodium hypochlorite and QMix in *Enterococcus faecalis* infected root canals, *Radiat. Eff. Defects Solids*, 2024, **179**(7–8), 1009–1016.
37 S. Damodaran and A. Paraf, *Food Proteins and Their Applications*, CRC Press, 2017.
38 C. Sarangapani, R. Thirumdas, Y. Devi, A. Trimukhe, R. R. Deshmukh and U. S. Annapure, Effect of low-pressure plasma on physico–chemical and functional properties of parboiled rice flour, *LWT–Food Sci. Technol.*, 2016, **69**, 482–489.
39 M. O. Iwe, U. Onyeukwu and A. N. Agiriga, Proximate, functional and pasting properties of FARO 44 rice, African yam bean and brown cowpea seeds composite flour, *Cogent Food Agric.*, 2016, **2**(1), 1142409.
40 A. Kheto, A. Mallik, R. Sehrawat, K. Gul and W. Routray, Atmospheric cold plasma induced nutritional & anti-nutritional, molecular modifications and in-vitro protein digestibility of guar seed (*Cyamopsis tetragonoloba* L.) flour, *Food Res. Int.*, 2023, **168**, 112790.
41 M. Hoque, C. McDonagh, B. K. Tiwari, J. P. Kerry and S. Pathania, Effect of Cold Plasma Treatment on the Packaging Properties of Biopolymer-Based Films: A Review, *Appl. Sci.*, 2022, **12**(3), 1346.
42 F. D. L. Almeida, R. S. Cavalcante, P. J. Cullen, J. M. Frias, P. Bourke, F. A. N. Fernandes, *et al.*, Effects of atmospheric cold plasma and ozone on prebiotic orange juice, *Innovative Food Sci. Emerging Technol.*, 2015, **32**, 127–135.
43 R. Mishra, A. Mishra, S. Jangra, S. Pandey, M. Chhabra and R. Prakash, Process parameters optimization for red globe grapes to enhance shelf-life using non-equilibrium cold plasma jet, *Postharvest Biol. Technol.*, 2024, **210**, 112778.
44 Y. Zhou, Y. Yan, M. Shi and Y. Liu, Effect of an Atmospheric Pressure Plasma Jet on the Structure and Physicochemical Properties of Waxy and Normal Maize Starch, *Polymers*, 2018, **11**(1), 8.
45 R. Thirumdas, A. Trimukhe, R. R. Deshmukh and U. S. Annapure, Functional and rheological properties of cold plasma treated rice starch, *Carbohydr. Polym.*, 2017, **157**, 1723–1731.
46 A. Sumathi, S. R. Ushakumari and N. G. Malleshi, Physico-chemical characteristics, nutritional quality and shelf-life of pearl millet based extrusion cooked supplementary foods, *Int. J. Food Sci. Nutr.*, 2007, **58**(5), 350–362.
47 R. Wongsagonsup, P. Deeyai, W. Chaiwat, S. Horrungsiwat, K. Leejariensuk and M. Suphantharika, Modification of tapioca starch by non-chemical route using jet atmospheric argon plasma, *Carbohydr. Polym.*, 2014, **102**, 790–798.
48 C. da Costa Pinto, E. A. Sanches, M. T. P. S. Clerici, S. Rodrigues, F. A. N. Fernandes and S. M. de Souza, Modulation of the Physicochemical Properties of Aria (*Goeppertia allouia*) Starch by Cold Plasma: Effect of Excitation Frequency, *Food Bioprocess Technol.*, 2023, **16**(4), 768–784.
49 P. Kaur and U. S. Annapure, Understanding the atmospheric cold plasma-induced modification of finger millet (*Eleusine coracana*) starch and its related mechanisms, *Int. J. Biol. Macromol.*, 2024, **268**, 131615.
50 N. N. Misra, B. Yadav, M. S. Roopesh and C. Jo, Cold Plasma for Effective Fungal and Mycotoxin Control in Foods: Mechanisms, Inactivation Effects, and Applications, *Compr. Rev. Food Sci. Food Saf.*, 2019, **18**(1), 106–120.
51 S. K. Pankaj, Z. Wan and K. M. Keener, Effects of Cold Plasma on Food Quality: A Review, *Foods*, 2018, **7**(1), 4), https://www.mdpi.com/2304-8158/7/1/4/htm.
52 S. Jaddu, R. C. Pradhan and M. Dwivedi, Effect of multipin atmospheric cold plasma discharge on functional properties of little millet (*Panicum miliare*) flour, *Innovative Food Sci. Emerging Technol.*, 2022, **77**, 102957.
53 X. Sun, A. S. M. Saleh, Z. Sun, X. Ge, H. Shen and Q. Zhang, Modification of multi-scale structure, physicochemical

properties, and digestibility of rice starch via microwave and cold plasma treatments, *LWT–Food Sci. Technol.*, 2022, **153**, 112483.

54 W. Gong, X. l. Guo, H. b. Huang, X. Li, Y. Xu and J. N. Hu, Structural characterization of modified whey protein isolates using cold plasma treatment and its applications in emulsion oleogels, *Food Chem.*, 2021, **356**, 129703.

55 J. K Joy, R. G. T. Kalaivendan, G. Eazhumalai, S. P. Kahar and U. S. Annapure, Effect of pin-to-plate atmospheric cold plasma on jackfruit seed flour functionality modification, *Innovative Food Sci. Emerging Technol.*, 2022, **78**, 103009.